International Journal of Mathematical, Engineering and Management Sciences
Vol. 8, No. 4, 595-611, 2023
https://doi.org/10.33889/IJMEMS.2023.8.4.034

Hierarchical Reliability Modelling and Analysis of Life Support System of Fighter Aircraft

Anubhav Tandon
Subir Chowdhary School of Quality and Reliability,
Indian Institute of Technology Kharagpur, Kharagpur, West Bengal, India.
Corresponding author: anubhav028@gmail.com

Vidhya Bhushan Verma
Subir Chowdhary School of Quality and Reliability,
Indian Institute of Technology Kharagpur, Kharagpur, West Bengal, India.
E-mail: vibu1225@gmail.com

Sanjay K. Chaturvedi
Subir Chowdhary School of Quality and Reliability,
Indian Institute of Technology Kharagpur, Kharagpur, West Bengal, India.
E-mail: skcrec@hijli.iitkgp.ac.in

(Received on February 15, 2023; Accepted on May 25, 2023)

Abstract
The paper proposes a hierarchical reliability modelling and assessment approach for a life support system (LSS) that provides oxygen to the pilot and is employed in a combat aircraft. The system has the primary function of generating oxygen onboard, and it has a backup gaseous oxygen tank as redundancy. An emergency oxygen bottle is also part of the ejection seat for emergency use. Both backup oxygen and emergency oxygen have a fixed capacity and a fixed duration of oxygen supply. Therefore, it is crucial to assess the reliability of the LSS to ensure its safety and effectiveness of this LSS during a mission by the combat aircraft. The proposed reliability model of LSS is developed as a two-level hierarchical model, that captures the inherent randomness in the operation of the system. At the lowest level of the hierarchy, Markov chains are used to model the events that may lead to the failure of the LSS. The events include the failure of individual components, the depletion of backup oxygen, and the depletion of emergency oxygen. The Markov chains consider the interactions between individual components and events during the mission profile. At the top level of the hierarchy, a fault tree is used to model the interactions between various events during the mission profile. The fault tree considers the interactions between individual events and the effects of redundancy on the reliability of the LSS. The results of the Markov chains at the lower level are exported to the higher level modelled via fault tree to find the overall system reliability. The reliability model is further extended to incorporate the deterministic nature of the LSS due to the fixed capacity of the backup tank and emergency bottle. The work addresses the modelling of six different scenarios of LSS operations. The modelling of these scenarios is achieved using Semi-Markov Processes (SMP), which allow the state holding time to be a general distribution.

Keywords- Hierarchical reliability modelling, Markov chains, Semi-Markov process, OBOGS.

Acronyms

BGMS	Breathing Gas Management System
BOS	Backup Oxygen System
ECU	Electronic Control Unit
EOS	Emergency Oxygen System
EPRD	Electronic Parts Reliability Data
FT	Fault Tree
LSS	Life Support System
MTTA	Mean Time to Absorption
MTTF	Mean Time to Failure
NPRD	Non-electronic Parts Reliability Data
OBOGS	On-Board Oxygen Generating System
RBD	Reliability Block Diagram
SMP	Semi-Markov Process
TPM	Transition Probability Matrix

Notation

β_{SW1}	Switching rate: 21,000 ft cabin altitude
β_{SW2}	Switching rate: Low to High cycle
β_{SW3}	Switching rate: Forced operation
β_{SW4}	Switching rate: Low cycle to BOS

β_{SW5}	Switching rate: High cycle to BOS	L_1	Expected time spent above 21,000 ft in a sortie
λ_O	Failure rate of Oxygen Sensor	L_2	Expected time when OBOGS is unable to meet oxygen concentration requirement
λ_{ECU}	Failure rate of ECU		
λ_{OBOGS}	Failure rate of OBOGS		
μ_{SW1}	Recovery rate: 21,000 ft cabin altitude	L_3	Expected time spent in a sortie in forced operation
μ_{SW2}	Recovery rate: High to Low cycle	L_B	BOS tank capacity in hours
μ_{SW3}	Recovery rate: From forced operation	L_E	EOS tank capacity in hours
μ_{SW4}	Recovery rate: BOS to OBOGS	P_{SW}	Probability of successful switching

1. Introduction

The On-Board Oxygen Generating System (OBOGS) is a critical component of the Life Support System (LSS) in modern fighter aircraft, which generates oxygen on demand and supplies it to the pilot/crew during a flight. The OBOGS system uses a molecular sieve to filter out nitrogen and other gases from the ambient air, leaving behind high-purity oxygen, which is then delivered to the pilot/crew through masks or other breathing apparatus. During the initial days of aviation, the oxygen was directly inhaled from the ambient atmosphere, and later came the gaseous oxygen tanks, followed by the liquid oxygen tanks. But this solution also had the limitation of having a fixed capacity and a limited duration. The problem is tackled through the idea and implementation of OBOGS coupled with a backup oxygen tank to alleviate such limitations and also increase system reliability and the safe return of the aircrew. The objective of this work is to model and analyze such critical systems from a reliability engineering perspective.

Obviously, the dynamic behaviour of such complex systems cannot be captured through ubiquitous reliability block/logic diagrams (RBD/RLD) or fault tree approaches alone. The proposed reliability model is, therefore, developed as a two-level hierarchy, which captures the inherent randomness in the operation of the system. At the lowest level of the hierarchy, Markov chains are used to model the events that may lead to the failure of the Life Support System (LSS). Semi-Markov Process (SMP) is shown to be a powerful technique for complex systems because of its ability to represent general sojourn times. Semi-Markov processes, a class of stochastic processes with memory, have emerged as powerful tools for modelling reliability systems due to their ability to capture both continuous and discrete states and transitions. Notwithstanding, the SMP, owing to its generic assumption form, is a useful tool for modelling the operation processes of numerous technical objects and systems. Hjelmgren et al. (1998), presented a reliability model consisting of separate independent Markov models for the control modules and the sensors of a single-engine aircraft Full Authority Digital Engine Control (FADEC). But the analysis was restricted to electronic parts only. Cao et al. (2002) presented a transient analysis of the minimum duration of outages for the RF (Radio Frequency) channel in cellular systems. The deterministic minimum duration gives rise to a stochastic process that is non-Markovian in nature. Yin et al. (2002) presented an application of SMP and Continuous Time Markov Chains (CTMC) to evaluate the availability of an uninterrupted power supply system. Two approximation models were proposed, wherein the first model employed SMP with the assumption that the battery unit would be fully recharged before the next failure occurred, and the second model used CTMC. Misra et al. (2012) presented an uncertainty analysis of the remote exploration and experimentation system by employing a three-stage hierarchical model to capture failure behaviour. At the lowest level, a Markov model captured the failure behaviour of the software subsystem. At the mid-level, the failure behaviour of individual components was captured using RBDs. The top-level model was a fault tree that captured the interactions between the individual components to provide overall system reliability. Mishra et al. (2010) presented a parts count-based reliability prediction of the LSS of a fighter aircraft, besides carrying out the FMEA and FMECA. The predicted failure rates in this work are used for the numerical results of this paper. Interested readers may refer to Misra (2012) and Trivedi and Bobbio (2017)

for not only a detailed description of Markov chains and SMP models but also numerous examples and references therein.

The rest of the paper is organized as follows: Section 2 covers a brief description of the system, wherein the deterministic nature of the system is explained along with the details of capacity, pressure thresholds, and control mechanisms. Section 3 describes the proposed two-level hierarchical reliability model of the LSS. Sub-sections 3.1 and 3.2 give the top and lower levels of the model. The overall reliability computation of the LSS is covered in Section 4 by taking the partial results of Sub-section 3.2. Section 5 gives the result and discussion. Finally, Section 6 concludes the work done in this paper.

2. Brief Description of LSS

The basic architecture of LSS is shown in Figure 1. The heart of the LSS is the Electronic Control Unit (ECU), whose major function is to control, monitor and coordinate the different functions of the LSS.

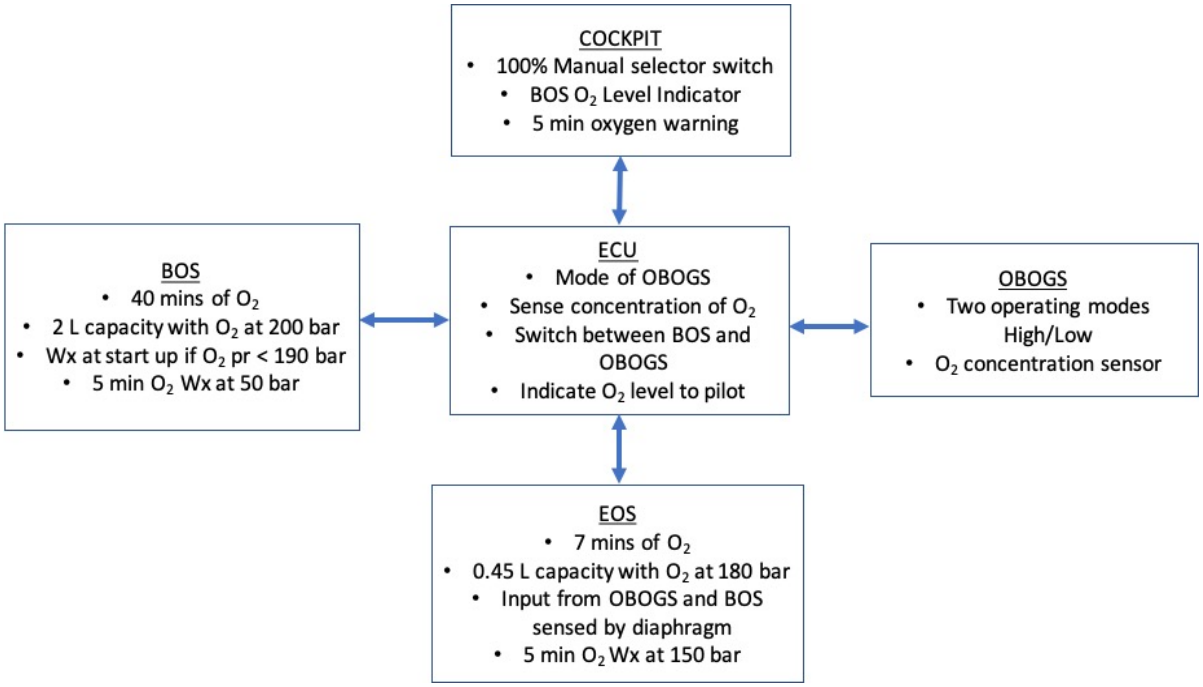

Figure 1. Basic block diagram of LSS.

The O_2 concentration sensor compares the concentration of oxygen from OBOGS with the reference concentration level of oxygen. This input from the oxygen sensor is taken by the ECU and compared with a look-up table containing the *altitude versus the level* of oxygen to maintain the required concentration. Depending on the level of needed oxygen concentration, the ECU switches to the low or high mode of the OBOGS modes. However, in the eventuality of not meeting the required concentration in high mode, the ECU switches to the backup oxygen system (BOS). This function of switching between high and low mode is achieved through the Breathing Gas Management System (BGMS), which is a solenoid valve used to select either OBOGS or BOS. The BOS cylinder capacity is usually about two liters filled with gaseous oxygen at a pressure of around 200 bar. It can supply 100% oxygen for roughly 40 minutes. In any OBOGS

failure condition, the BGMS automatically selects BOS. Nonetheless, the BOS can also be selected manually by the pilot through a '100% /Normal' selection switch inside the cockpit. When the cabin altitude reaches a certain altitude, say, 21,000 feet (aircraft altitude[1] 50,000 feet), the ECU may command the BGMS to switch to BOS from OBOGS. The BOS cylinder pressure is continuously monitored by the ECU through a pressure sensor. When the pilot starts the engine and if the pressure inside a typical BOS cylinder is, say, less than about 190 bar then the ECU gives a warning signal to the pilot that BOS has less oxygen, and when the BOS cylinder pressure reaches around 50 bar it gives another warning signal that only ~5 minutes' oxygen is left in the BOS cylinder.

The EOS cylinder is located inside the pilot seat. The functioning of the Emergency Oxygen System (EOS) is similar to that of the BOS, except for some differences in constructional features. Here, the EOS cylinder capacity is usually much less, e.g., 0.45 liters containing oxygen at a pressure of roughly around 180 bar or so, which is usually exhausted within seven minutes. the EOS comes into action when both OBOGS and BOS fail or there is a requirement for emergency ejection. The input from OBOGS or BOS is sensed by a diaphragm with a threshold of about 0.8 bar below which it activates EOS. When the cylinder pressure falls below 150 bar, a 5-minute warning signal is received by the pilot.

3. Proposed Hierarchical Reliability Model

The system reliability model is developed as a 2-level hierarchy (illustrated in Figure 2). The reliability model of LSS captures the failure behavior of the LSS system. Reliability models are defined separately for different events, which are then combined into an overall system model. At the top level, the system is modeled using a fault-tree which considers the interactions between various events during the mission profile. The lower level captures the event-level failures while considering the interactions between individual components. The reliability measures computed at a lower level using Markov chains become an input to the top level.

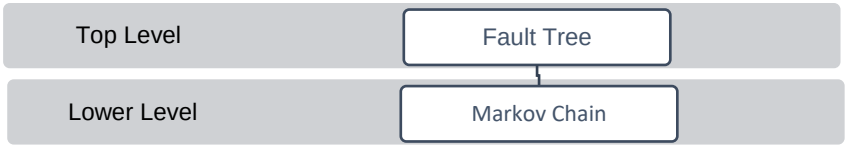

Figure 2. Two-level hierarchical model.

3.1 LSS Top Level Model using Fault Tree

The fault tree model for the top level of the proposed hierarchical model is illustrated in Figure 3. The LSS architecture permits the switching from OBOGS to BOS under three conditions, *viz.*, (i) any failure in OBOGS, (ii) switching failure in software logic, and, (iii) manually or forced switch. These become in series configuration as either condition will lead to a switchover to BOS. Further, the OBOGS has three major sub-components, which may lead to hardware failure: oxygen sensor failure, OBOGS failure, and ECU failure. These sub-components are reliable reliability-wise in a series configuration, and constitute the hardware failure. Similarly, the switching failure in software logic can be due to either high-low switching failure or altitude switching failure. These, in series, constitute the switching failure. The forced switch is at the pilot discretion (in case the pilot feels uneasy due to a lack of oxygen) to switch to BOS.

[1] Aircraft altitude is the height above sea level that an aircraft is flying, while cabin altitude refers to the pressurized altitude maintained inside the aircraft's cabin to ensure passenger comfort and safety.

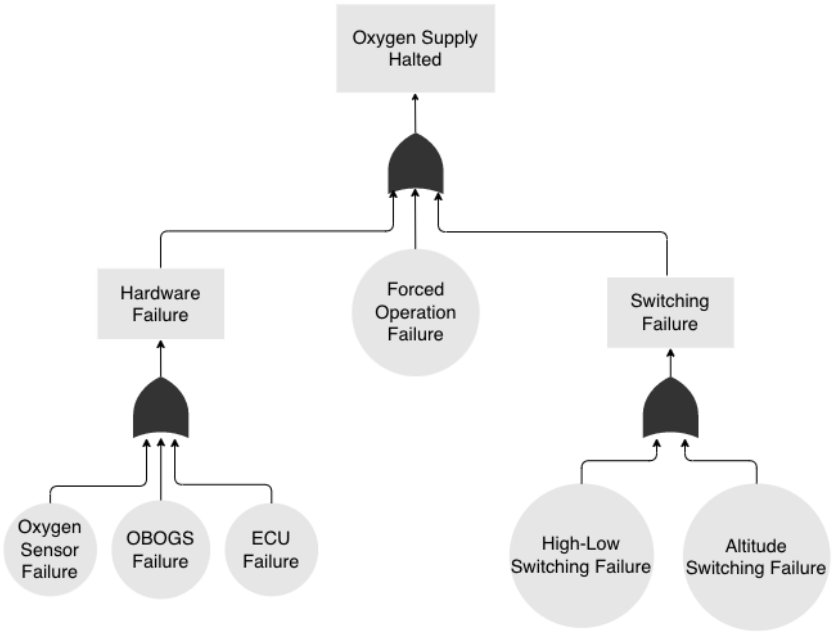

Figure 3. Top-level fault tree model of LSS**.**

3.2 LSS Lower Level Model using Semi Markov Process

Here, we propose the models under different scenarios during the operation of LSS:

3.2.1 Case I: Altitude Switching Failure

The state transition diagram for altitude switching is illustrated in Figure 4. The behavior is modelled using a 5-state SMP. The states in this model are: O represents oxygen supplied by OBOGS, and B' state represents oxygen supplied by BOS when the aircraft is, say, above 21,000 ft cabin altitude. It is assumed that in state B', there is no failure in switching software. Once the aircraft is again below 21,000 ft cabin altitude, state transits from B' to O. State B represents oxygen supplied by BOS when the software failed to switch during an altitude change. State E represents oxygen supplied by EOS. State D represents the state where the oxygen supply is halted. The transitions from SMP states are deterministic and are modelled using unit step functions with respective oxygen tank capacities in hours as their threshold.

Therefore, the Transition Probability Matrix (TPM) embedded DTMC is:

$$P = \begin{array}{c} \\ O \\ B' \\ B \\ E \\ D \end{array} \begin{array}{c} \begin{array}{ccccc} O & B' & B & E & D \end{array} \\ \begin{bmatrix} 0 & P_{O,B'} & P_{O,B} & 0 & 0 \\ P_{B',O} & 0 & P_{B',B} & 0 & 0 \\ 0 & 0 & 0 & 1 & 0 \\ 0 & 0 & 0 & 0 & 1 \\ 0 & 0 & 0 & 0 & 1 \end{bmatrix} \end{array}.$$

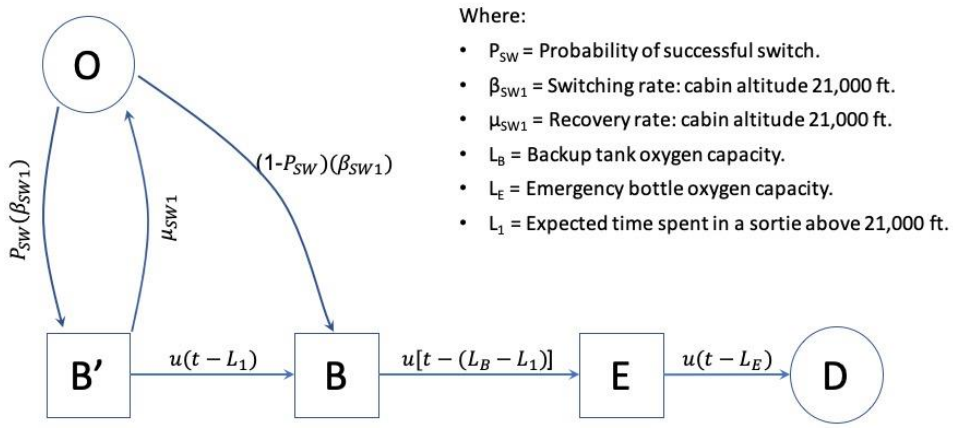

Figure 4. SMP model for altitude switching.

The entries of the TPM are determined by the minimum of the transition time (Cao et al., 2002):

$$p_{O,B'} = \int_0^\infty \big(1 - F_B(t)\big) dF_{B'}(t) \tag{1}$$

$$p_{O,B'} = \int_0^\infty e^{-[(1-P_{SW})\beta_{SW1}]t} dF_{B'}(t).$$

$$p_{O,B'} = \int_0^\infty e^{-[(1-P_{SW})\beta_{SW1}]t}.(P_{SW}\beta_{SW1})e^{-[P_{SW}\beta_{SW1}]t} dt.$$

$$p_{O,B'} = P_{SW}\beta_{SW1}\int_0^\infty e^{-[(1-P_{SW})\beta_{SW1}+(P_{SW}\beta_{SW1})]t} dt.$$

$$p_{O,B'} = \frac{P_{SW}\beta_{SW1}}{P_{SW}\beta_{SW1}+(1-P_{SW})\beta_{SW1}} \tag{2}$$

Similarly,

$$p_{O,B} = \frac{(1-P_{SW})\beta_{SW1}}{P_{SW}\beta_{SW1}+(1-P_{SW})\beta_{SW1}} \tag{3}$$

Now,

$$p_{B',O} = \int_0^t 1 - u(\tau - L_1) dF_O(\tau) \tag{4}$$

$$p_{B',O} = [1 - e^{-\mu_{SW1}t}] - \int_{L_1}^t \mu_{SW1} e^{-\mu_{SW1}\tau} d\tau.$$

$$p_{B',O} = [1 - e^{-\mu_{SW1}t}] - [-e^{-\mu_{SW1}t} + e^{-\mu_{SW1}L_1}].$$

$$p_{B',O} = [1 - e^{-\mu_{SW1}L_1}] \tag{5}$$

Hence,

$$p_{B',B} = e^{-\mu_{SW1}L_1} \tag{6}$$

We have the following TPM from Equations (2), (3), (5) and (6):

$$P = \begin{array}{c} \\ O \\ B' \\ B \\ E \\ D \end{array} \begin{array}{c} \begin{array}{cccccc} O & B' & B & E & D \end{array} \\ \begin{bmatrix} 0 & \frac{P_{SW}\beta_{SW1}}{P_{SW}\beta_{SW1}+(1-P_{SW})\beta_{SW1}} & \frac{(1-P_{SW})\beta_{SW1}}{P_{SW}\beta_{SW1}+(1-P_{SW})\beta_{SW1}} & 0 & 0 \\ 1-e^{-\mu_{SW1}L_1} & 0 & e^{-\mu_{SW1}L_1} & 0 & 0 \\ 0 & 0 & 0 & 1 & 0 \\ 0 & 0 & 0 & 0 & 1 \\ 0 & 0 & 0 & 0 & 1 \end{bmatrix} \end{array}.$$

The expected number of visits V_j to state j until absorption is given by Kao (1974), Kemeny and Snell, (1983), Trivedi and Bobbio, (2017),

$$V_j = \alpha_j + \sum_{i=1}^{n-1} V_i p_{ij} \qquad j = 1,2,\ldots.n \tag{7}$$

where, α_j is the initial probability of state j, p_{ij} is the probability of transition from i to j and state n is the absorbing state. In vector form,

$$V = \alpha + VP_u \tag{8}$$

where, $\alpha = [\alpha_j]$ is the initial probability vector and $V = [V_j]$ is the vector of the expected number of visits in each state. P_u is the $(n-1 \times n-1)$ partition matrix of TPM over the transient states and is a sub-stochastic matrix. By computing the average number of visits to state j, the mean time to absorption is given as:

$$MTTA = \sum_{j=1}^{n-1} V_j h_j \tag{9}$$

where, h_j is the mean state holding time in state j.

Now for the altitude switching SMP model, assuming the initial probability $\alpha_O = 1$, we have,

$$V_O = 1 + V_{B'}(1 - e^{-\mu_{SW1}L_1}) \tag{10}$$

$$V_{B'} = V_O \cdot \frac{P_{SW}\beta_{SW1}}{P_{SW}\beta_{SW1}+(1-P_{SW})\beta_{SW1}} \tag{11}$$

For states B and E, since they have no return path in the model and they are deterministic, the number of visits to the state will be 1,

$V_B = 1$, and $V_E = 1$, Now solving Equation (10),

$V_O = 1 + V_{B'}(1 - e^{-\mu_{SW1}L_1})$,

$$V_O = 1 + V_O \cdot \frac{P_{SW}\beta_{SW1}}{P_{SW}\beta_{SW1}+(1-P_{SW})\beta_{SW1}}(1 - e^{-\mu_{SW1}L_1}),$$

$$V_O = \frac{1}{1-\frac{P_{SW}\beta_{SW1}}{P_{SW}\beta_{SW1}+(1-P_{SW})\beta_{SW1}}(1-e^{-\mu_{SW1}L_1})} \tag{12}$$

$H_i(t)$ is the sojourn time distribution of state i. Now mean sojourn time in state i is given by Pievatolo and Valad`e (2003),

$$h_i(t) = \int_0^\infty \prod_{j=1}^{n} \Big(1 - F_j(t)\Big)\, dt \tag{13}$$

Therefore, the mean sojourn times for all states of the altitude switching model are

$$h_O = \int_0^\infty e^{-[(1-P_{SW})\beta_{SW_1}]t}.e^{-(P_{SW}\beta_{SW_1})t}dt,$$

$$h_O = \int_0^\infty e^{-[(1-P_{SW})\beta_{SW_1}+(P_{SW}\beta_{SW_1})]t}dt,$$

$$h_O = \frac{1}{P_{SW}\beta_{SW_1}+(1-P_{SW})\beta_{SW_1}} \quad (14)$$

For state B',

$$h_{B'} = \int_0^\infty e^{-\mu_{SW_1}t}\big(1-u(t-L_1)\big)dt,$$

$$h_{B'} = \int_0^\infty e^{-\mu_{SW_1}t}dt - \int_{L_1}^\infty e^{-\mu_{SW_1}t}dt,$$

$$h_{B'} = \frac{1-e^{-\mu_{SW_1}L_1}}{\mu_{SW_1}} \quad (15)$$

Finally, for deterministic states, B and E, their mean state holding times become the capacity of BOS and EOS respectively. As the aircraft is expected to spend 1 minute above 21,000 ft (values given in Table 1 below) where BOS will supply oxygen, the remaining capacity, *i.e.*, 39 minutes is taken as the mean state holding time for state B. Likewise, the state holding time for state E would be 7-minutes as the EOS has a capacity of 7 minutes, i.e., $h_B = 39\ mins$ and $h_E = 7\ mins$.

The assumed parameters used in the LSS reliability model are summarized in Table 1[2]; the failure rates have been taken under airborne conditions from available databases such as Mil-HDBK 217F N2, NPRD/EPRD, NSWC, and Relex® library. Therefore, taking values from Table 1 (given below) the MTTF (for this system MTTF=MTTA as it is non-repairable in the air during the mission time) is computed using Equation (9).

$$MTTA = MTTF = V_O h_O + V_{B'} h_{B'} + V_B h_B + V_E h_E = 1000.7993\ hrs.$$

Reliability for altitude switching model for an assumed mission time of 3 hours,

$$R = e^{-\frac{1}{MTTA}t} \quad (16)$$

$$R = 99.70\%.$$

Table 1. Assumed values of LSS model.

Symbol	Meaning	Value	Unit
λ_O	Failure rate of Oxygen Sensor	3.64 x 10^{-4}	hr^{-1}
λ_{OBOGS}	Failure rate of OBOGS	2.16 x 10^{-4}	hr^{-1}
λ_{ECU}	Failure rate ECU	1.74 x 10^{-4}	hr^{-1}
P_{SW}	Probability of successful switching	0.98	--
β_{SW1}	Switching rate: cabin altitude 21,000 ft	0.001	hr^{-1}
β_{SW2}	Switching rate: Low to High cycle	0.1	hr^{-1}
β_{SW3}	Switching rate: Forced operation	0.005	hr^{-1}
μ_{SW1}	Recovery rate: cabin altitude 21,000 ft	0.001	hr^{-1}
μ_{SW2}	Recovery rate: High to Low cycle	0.1	hr^{-1}
μ_{SW3}	Recovery rate: Forced Operation	0.005	hr^{-1}
μ_{SW4}	Recovery rate: BOS to OBOGS	0.1	hr^{-1}
L_1	Expected time spent above 21,000 ft in a sortie	1	min
L_2	Expected time when OBOGS is unable to meet oxygen concentration requirement	5	min
L_3	Expected time spent in a sortie in forced operation	1	min

[2] *The failure rates are taken from previous work on reliability prediction on the same system (Table 1 pp. 22 of Mishra et al., 2010). The other values are assumed and real-world values can be obtained specific to the aircraft the LSS is installed on.*

3.2.2 Case II: High-Low Switching

The state transition diagram for High-Low switching is illustrated in Figure 5. The behavior is modelled using a 6-state SMP. The state O_L represents the OBOGS working in low mode. In the event of a low concentration of oxygen, the ECU commands the high mode of OBOGS which is represented by state O_H. The State B' represents oxygen supplied by BOS when even the high mode is unable to generate the required concentration of oxygen. State B represents oxygen supplied by BOS once software encounters a failure. Here, State E represents oxygen supplied by the EOS. State D represents the absorbing state where the oxygen supply is halted.

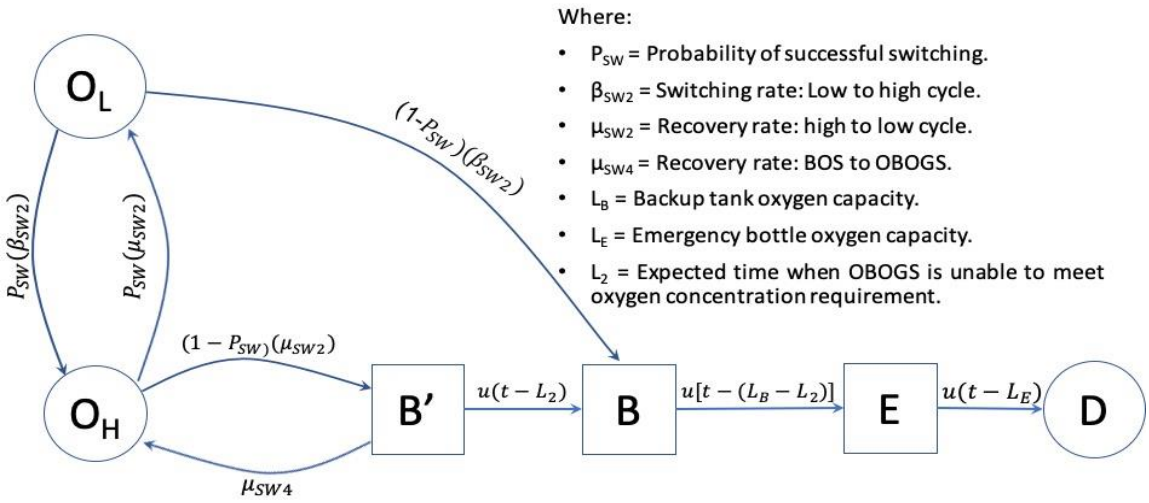

Figure 5. SMP model for high-low switching.

We have the following transition probability matrix for High-Low switching by finding the minimum of the transition times,

$$P = \begin{bmatrix} 0 & \frac{P_{SW}\beta_{SW2}}{P_{SW}\beta_{SW2}+(1-P_{SW})\beta_{SW2}} & 0 & \frac{(1-P_{SW})\beta_{SW2}}{P_{SW}\beta_{SW}+(1-P_{SW})\beta_{SW2}} & 0 & 0 \\ \frac{P_{SW}\beta_{SW2}}{P_{SW}\beta_{SW2}+(1-P_{SW})\beta_{SW2}} & 0 & \frac{(1-P_{SW})\beta_{SW2}}{P_{SW}\beta_{SW}+(1-P_{SW})\beta_{SW2}} & 0 & 0 & 0 \\ 0 & 1-e^{-\mu_{SW4}L_2} & 0 & e^{-\mu_{SW4}L_2} & 1 & 0 \\ 0 & 0 & 0 & 0 & 1 & 0 \\ 0 & 0 & 0 & 0 & 0 & 1 \\ 0 & 0 & 0 & 0 & 0 & 1 \end{bmatrix}.$$

Now for the High-Low switching SMP model, assuming the initial probability $\alpha_{O_L} = 1$, we have from Equation (7),

$$V_{O_L} = 1 + V_{O_H}\frac{P_{SW}\mu_{SW2}}{P_{SW}\mu_{SW2}+(1-P_{SW})\mu_{SW2}} \tag{17}$$

$$V_{O_H} = V_{O_L}\frac{P_{SW}\beta_{SW2}}{P_{SW}\beta_{SW2}+(1-P_{SW})\beta_{SW2}} + V_{B'}(1-e^{-\mu_{SW4}L_2}) \tag{18}$$

$$V_{B'} = V_{O_H}\frac{(1-P_{SW})\mu_{SW2}}{P_{SW}\mu_{SW2}+(1-P_{SW})\mu_{SW2}} \tag{19}$$

$$V_B = V_{O_L} \frac{(1-P_{SW})\beta_{SW_2}}{P_{SW}\beta_{SW_2}+(1-P_{SW})\beta_{SW_2}} + V_{B'}(e^{-\mu_{SW_4}L_2}) \quad (20)$$

$V_E = 1$ and $V_D = 1$.

The state holding times for the SMP become using Equation (12),

$$h_{O_L} = \frac{1}{P_{SW}\beta_{SW_2}+(1-P_{SW})\beta_{SW_2}} \quad (21)$$

$$h_{O_H} = \frac{1}{P_{SW}\mu_{SW_2}+(1-P_{SW})\mu_{SW_2}} \quad (22)$$

$$h_{B'} = \frac{(1-e^{-\mu_{SW_4}L_2})}{\mu_{SW_4}} \quad (23)$$

For state B in this case, the expected time for which the OBOGS is unable to meet the oxygen requirement is 5 minutes (refer Table 1). Hence state holding time becomes 35 minutes. State E remains the same as in the previous case,

$$h_B = 35\ mins, \text{ and } h_E = 7\ mins.$$

Hence, the mean time to failure using values from Table 1 and Equation (9),

$$MTTF = 502.8036\ hrs.$$

Reliability for high-low switching model for an assumed mission time of 3 hours using Equation (15),

$$R = 99.40\%.$$

3.2.3 Case III: Oxygen Sensor Failure

The state transition diagram for the oxygen sensor is illustrated in Figure 6. The failure behavior of the oxygen sensor is modelled using a 4-state SMP. The state O represents oxygen supplied by OBOGS. The B state represents oxygen supplied by BOS after the failure of the oxygen sensor, E state represents supply from EOS. State D represents the absorbing state where the oxygen supply is halted. Let the transition from O to B is governed by an exponential distribution with failure rate λ_O. The transition from B to E and E to D is governed by deterministic distribution with parameter L_B and L_E respectively (time to exhaustion for BOS and EOS).

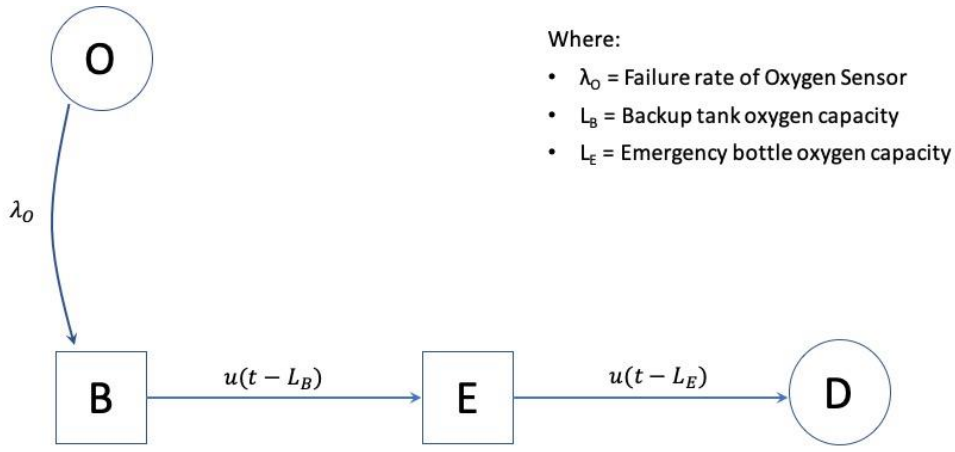

Figure 6. SMP model for oxygen sensor.

We have the following transition probability matrix, since all states have no return path,

$$P = \begin{array}{c} \\ O \\ B \\ E \\ D \end{array} \begin{array}{c} \begin{array}{cccc} O & B & E & D \end{array} \\ \begin{bmatrix} 0 & 1 & 0 & 0 \\ 0 & 0 & 1 & 0 \\ 0 & 0 & 0 & 1 \\ 0 & 0 & 0 & 1 \end{bmatrix} \end{array}.$$

Now for the oxygen sensor SMP model, assuming the initial probability $\alpha_O = 1$, using Equation (7) we have,

$$V_O = 1, V_B = 1 \text{ and } V_E = 1.$$

The mean state holding times for the SMP become,

$$h_O = \frac{1}{\lambda_O}, h_B = 40\ mins \text{ and } h_E = 7\ mins.$$

Finally, taking values from Table 1, the mean time to failure is computed using Equation (9),

$$MTTF = 2749.8577\ hrs.$$

Reliability for Oxygen sensor model for an assumed mission time of 3 hours using Equation (15),

$$R = 99.89\%.$$

3.2.4 Case IV: OBOGS Failure

The state transition diagram for OBOGS failure is illustrated in Figure 7. The failure behavior of the OBOGS is modelled using a 4-state SMP. The state O represents oxygen supplied by OBOGS. The state B represents oxygen supplied by the BOS after the failure of the OBOGS, E state represents supply from EOS. The state D represents the absorbing state where the oxygen supply is halted. It is assumed that the transition from state O to state B is governed by an exponential distribution with failure rate λ_{OBOGS}. The transition from B to E and E to D is governed by deterministic distribution with parameter L_B and L_E respectively (time to exhaustion for BOS and EOS).

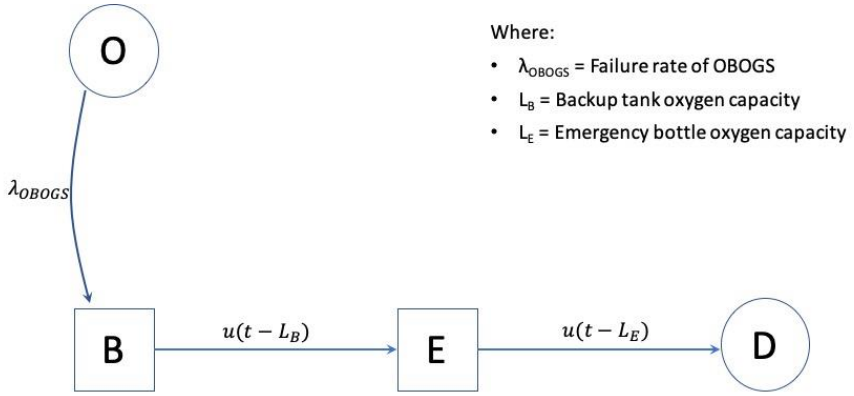

Figure 7. SMP model for OBOGS.

Now, for the OBOGS SMP model everything remains the same as the previous case except for the value of the failure rate. Assuming the initial probability $\alpha_O = 1$, we have the mean time to failure using values from Table 1 and Equation (9),

$$MTTF = 4637.8171\ hrs.$$

And, reliability for the OBOGS model for an assumed mission time of 3 hours using Equation (15),

$$R = 99.93\%.$$

3.2.5 Case V: ECU Failure

The state transition diagram for ECU failure is illustrated in Figure 8. The failure behavior of ECU is modelled by using a 4-state SMP. The state O represents oxygen supplied by OBOGS. The state B represents oxygen supplied by BOS after the failure of ECU, E state represents supply from EOS. State D represents the absorbing state where the oxygen supply is halted. The transition from state O to state B is governed by an exponential distribution with failure rate λ_{ECU}. The transition from B to E and E to D is governed by deterministic distribution with parameter L_B and L_E respectively (time to exhaustion for BOS and EOS).

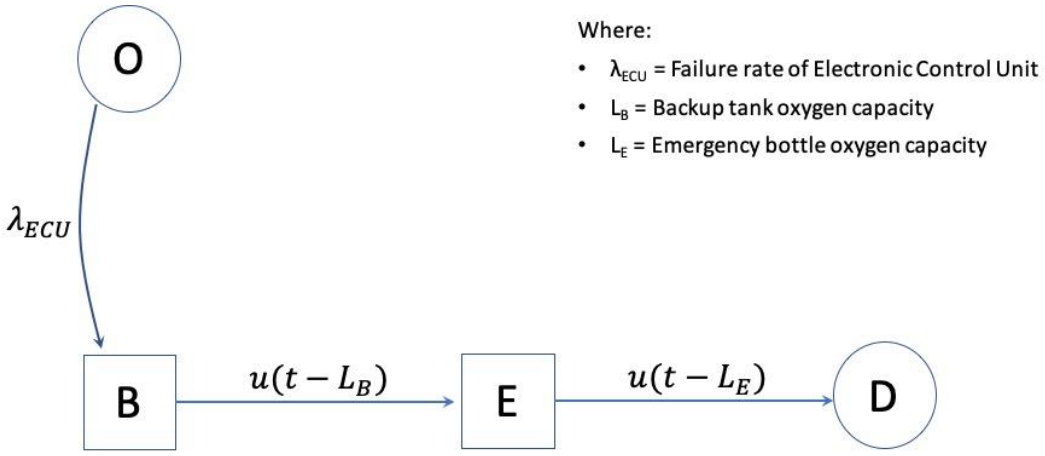

Figure 8. SMP model for ECU.

Now, for the ECU SMP model, assuming the initial probability $\alpha_O = 1$, we have the mean time to failure using values from Table 1,

$$MTTF = 5750.2095\ hrs.$$

And, the reliability for the ECU model for an assumed mission time of 3 hours using Equation (15),

$$R = 99.94\%.$$

3.2.6 Case VI: Forced Operation

The state transition diagram for forced operation is illustrated in Figure 9. The behavior is modelled using a 5-state SMP. The state O represents oxygen supplied by OBOGS. B' state represents oxygen supplied by BOS when the pilot manually selects BOS. It is to be noted that in state B' there is no failure in the system. Once the pilot again selects OBOGS, state transitions take place from state B' to state O. State B represents oxygen supplied by BOS when switching fails after manual selection. State E represents oxygen supplied by EOS. The state D represents the absorbing state where oxygen supply is halted. The transitions from SMP states is deterministic and are modelled using unit step functions with respective oxygen tank capacities in hours as their threshold.

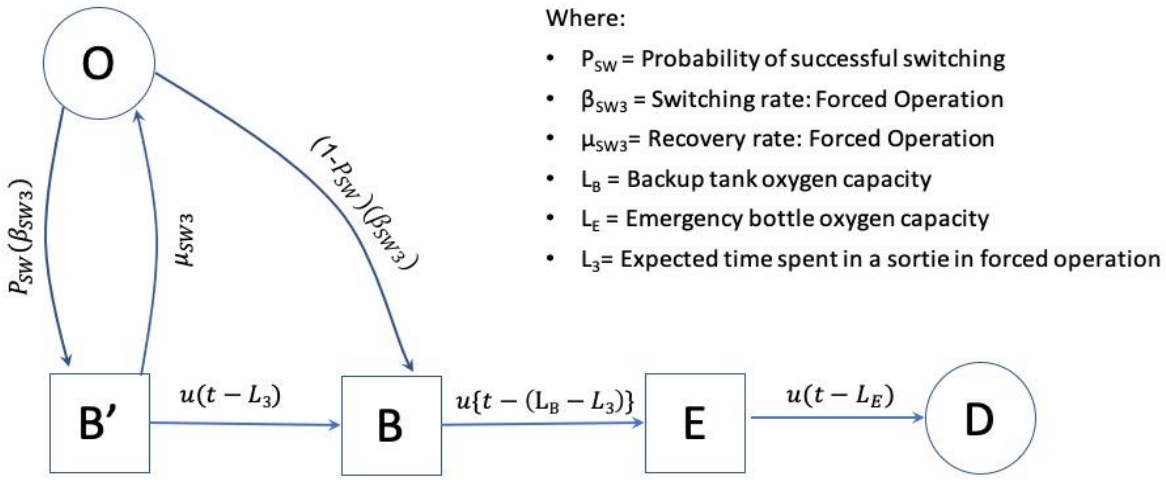

Figure 9. SMP model for forced operation.

The entries of the TPM of the embedded DTMC are as follows:

$$p_{O,B\prime} = \int_0^\infty (1-F_B)dF_{B'}(t) \tag{24}$$

$$p_{O,B\prime} = \int_0^\infty e^{-[(1-P_{SW})\beta_{SW3}]t} dF_{B'}(t),$$

$$p_{O,B\prime} = \int_0^\infty e^{-[(1-P_{SW})\beta_{SW3}]t}.(P_{SW}\beta_{SW3})e^{-[P_{SW}\beta_{SW3}]t}dt,$$

$$p_{O,B\prime} = P_{SW}\beta_{SW3}\int_0^\infty e^{-[(1-P_{SW})\beta_{SW3}+(P_{SW}\beta_{SW3})]t}dt,$$

$$p_{O,B'} = \frac{P_{SW}\beta_{SW3}}{P_{SW}\beta_{SW3}+(1-P_{SW})\beta_{SW3}} \tag{25}$$

Similarly,

$$p_{O,B} = \frac{(1-P_{SW})\beta_{SW3}}{P_{SW}\beta_{SW3}+(1-P_{SW})\beta_{SW3}} \tag{26}$$

Now,

$$p_{B',O} = \int_0^t 1-u(\tau-L_3)dF_O(\tau) \tag{27}$$

$$p_{B',O} = \int_0^t 1-u(\tau-L_3)\mu_{SW3}e^{-\mu_{SW3}\tau}d\tau,$$

$$p_{B',O} = [1-e^{-\mu_{SW3}t}] - \int_{L_3}^t \mu_{SW3}e^{-\mu_{SW3}\tau}d\tau,$$

$$p_{B',O} = [1-e^{-\mu_{SW3}t}] - [-e^{-\mu_{SW3}t}+e^{-\mu_{SW3}L_3}],$$

$$p_{B',O} = [1-e^{-\mu_{SW3}L_3}]. \tag{28}$$

Hence,

$$p_{B',B} = e^{-\mu_{SW3}L_3} \tag{29}$$

We have the following TPM,

$$P = \begin{array}{c} \\ O \\ B' \\ B \\ E \\ D \end{array} \begin{array}{c} \begin{array}{cccccc} O & B' & B & E & D \end{array} \\ \begin{bmatrix} 0 & \frac{P_{SW}\beta_{SW3}}{P_{SW}\beta_{SW3}+(1-P_{SW})\beta_{SW3}} & \frac{(1-P_{SW})\beta_{SW3}}{P_{SW}\beta_{SW3}+(1-P_{SW})\beta_{SW3}} & 0 & 0 \\ 1-e^{-\mu_{SW3}L_3} & 0 & e^{-\mu_{SW3}L_3} & 0 & 0 \\ 0 & 0 & 0 & 1 & 0 \\ 0 & 0 & 0 & 0 & 1 \\ 0 & 0 & 0 & 0 & 1 \end{bmatrix} \end{array}.$$

Now for the forced operation SMP model, assuming the initial probability $\alpha_O = 1$, we have using Equation (7):

$$V_O = 1 + V_{B'}(1 - e^{-\mu_{SW3}L_3}) \tag{30}$$

$$V_{B'} = V_O \cdot \frac{P_{SW}\beta_{SW3}}{P_{SW}\beta_{SW3}+(1-P_{SW})\beta_{SW3}} \tag{31}$$

$$V_B = 1.$$

$$V_E = 1.$$

Now, on solving Equation (29),

$$V_O = 1 + V_O \cdot \frac{P_{SW}\beta_{SW3}}{P_{SW}\beta_{SW3}+(1-P_{SW})\beta_{SW3}}(1 - e^{-\mu_{SW3}L_3}).$$

$$V_O = \frac{1}{1-\frac{P_{SW}\beta_{SW3}}{P_{SW}\beta_{SW3}+(1-P_{SW})\beta_{SW3}}(1-e^{-\mu_{SW3}L_3})}.$$

Therefore, mean sojourn times for all states of the forced operation model using Equation (12) are:

$$h_O = \int_0^\infty e^{-[(1-P_{SW})\beta_{SW3}]t} . e^{-(P_{SW}\beta_{SW3})t} dt,$$

$$h_O = \int_0^\infty e^{-[(1-P_{SW})\beta_{SW3}+(P_{SW}\beta_{SW3})]t} dt,$$

$$h_O = \frac{1}{P_{SW}\beta_{SW3}+(1-P_{SW})\beta_{SW3}} \tag{32}$$

For state *B'*,

$$h_{B'} = \int_0^\infty e^{-\mu_{SW3}t}(1 - u(t - L_3))dt,$$

$$h_{B'} = \int_0^\infty e^{-\mu_{SW3}t} dt - \int_{L_3}^\infty e^{-\mu_{SW3}t} dt,$$

$$h_{B'} = \frac{1-e^{-\mu_{SW3}L_3}}{\mu_{SW3}} \tag{33}$$

and,

$$h_B = 39\ mins, \text{ and } h_E = 7\ mins.$$

Finally, taking values from Table 1, the MTTF is computed using Equation (9),

$$MTTF = 200.7993\ hrs.$$

Reliability for forced operation model for a mission time of 3 hours using Equation (15),

$$R = 98.51\%.$$

4. Overall System Reliability

The overall system reliability is computed by importing results from the lower-level Markov chains to the higher ones. The hardware failure is computed from the results of the Oxygen sensor, OBOGS, and ECU SMP models. Hence for hardware failure for an assumed mission time of 3 hours:

$$R_{Hardware} = R_O \times R_{OBOGS} \times R_{ECU} = 99.77\%.$$

Similarly, for software failures: $R_{Software} = R_{High-Low} \times R_{Altitude\ Switching} = 99.10\%$.

From the fault tree (illustrated in Figure 3), the overall system comprises hardware failures, forced operation, and software failures. Hence the overall system reliability for a mission time of 3 hours is given by:

$$R_{Overall} = R_{Hardware} \times R_{Forced\ Operation} \times R_{Software} = 97.41\%.$$

5. Result and Discussion

In this paper, a 2-level hierarchical model of an oxygen generation system used in military aircraft has been proposed to analyze the reliability of a life support system employed in a combat aircraft. The top level of the proposed model was a fault tree while the lowest level consisted of Markov chains. Six situations have been considered under the different scenarios during the operation of LSS. The overall system reliability was computed by importing the results from the lowest-level Markov chains. The results showed that the overall system reliability for predicted failure rates from databases and a typical flight time of three hours was estimated to be 97.41%.

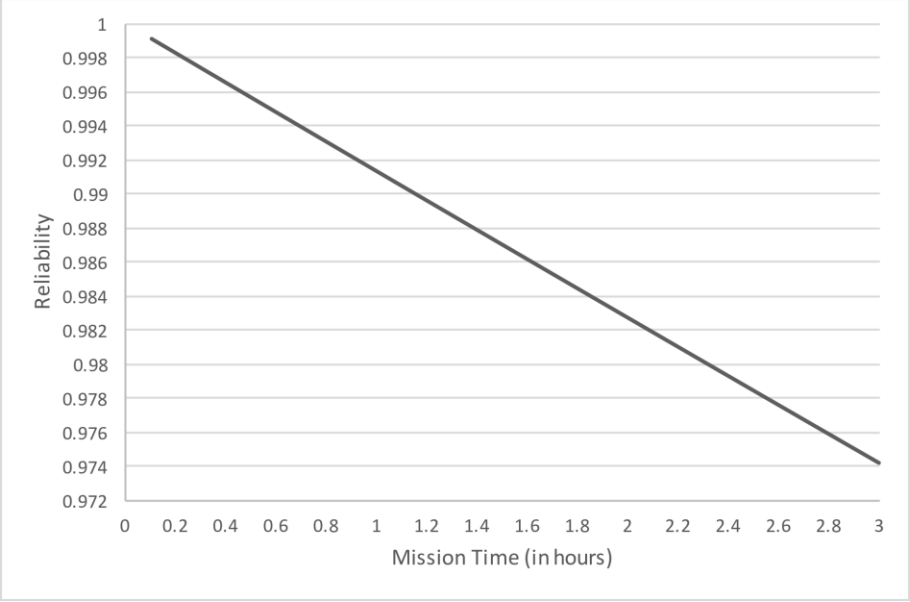

Figure 10. System reliability for different mission time.

In Figure 10, we plot the overall system reliability curve for a single mission time. The assumed flight time is usually short in comparison to the MTTF of the components, meaning that the expected time for a component to fail is much longer than the flight time. As a result, the effect of the component failure rate on the overall system reliability is not significant over the assumed mission time, and the reliability plot appears to be linear.

This observation is important because it indicates that the overall system reliability is not sensitive to the failure rate of the individual components for the assumed mission time. However, it should be noted that for longer mission times, the effect of the component failure rate on the overall system reliability may become more significant.

The hierarchical approach proposed in this paper was found to be more effective in capturing the real scenarios of the oxygen generation system in comparison to ubiquitous RBD or FT alone. This is because the model considered the dependencies of various subsystems resulting in a better estimate of the overall system reliability emphasizing the need for a hierarchical model.

6. Conclusion

In this paper, a 2-level hierarchical model has been proposed with the top level as a fault tree, and the basic events of the fault tree were modelled using Markov chains. The SMP has been used, as it permits the state holding times following a general distribution and capture the realistic nature of the system. The results from the lowest level Markov chains were imported to top-level fault tree to obtain the overall system reliability, considering the dependencies of various subsystems. If the dependencies of the subsystems are not considered, then with the same failure rates data of OBOGS, the reliability turned out to be 99.93%. However, the overall system reliability considering dependencies for an assumed flight time of 3 hours, is estimated to be 97.41%. This significant variation in reliability emphasizes the importance of considering dependencies among subsystems while analyzing the reliability of a life-critical system. In conclusion, we can say that the hierarchical approach captures the real scenarios in a better manner than the conventional models such as RBD or FT alone. In conclusion, we can say that the hierarchical approach is a better approach to modelling such systems than conventional models such as RBD or FT alone.

While the proposed model provided a good approximation of the overall system reliability of the LSS, there are several areas for future improvement. Firstly, the proposed model assumes that the failure rates of the various components are constant over time, which may not be true in practice. The use of time-varying failure rates could provide a more accurate estimate of the system's reliability. The model presented in this paper does not consider the effects of maintenance and repair on system reliability. The inclusion of maintenance and repair models could help predict the impact of maintenance activities on system reliability and inform maintenance scheduling decisions. Further, the integration of semi-Markov processes with other modelling formalisms (e.g., Bayesian networks, Petri nets) could also be explored for modelling the dynamic scenarios of such systems critical to defense applications.

Conflict of Interest

The authors confirm that there is no conflict of interest to declare for this publication.

Acknowledgments

This research did not receive any specific grant from funding agencies in the public, commercial, or not-for-profit sectors. The authors would like to thank the editor and anonymous reviewers for their comments that help improve the quality of this work.

References

Cao, Y., Sun, H., Trivedi, K., & Han, J. (2002). System availability with non-exponentially distributed outages. *IEEE Transactions on Reliability*, *51*(2), 193-198.

Hjelmgren, K., Svensson, S., & Hannius, O. (1998). Reliability analysis of a single-engine aircraft FADEC. In *Annual Reliability and Maintainability Symposium. 1998 Proceedings. International Symposium on Product Quality and Integrity* (pp. 401-407). IEEE. Anaheim, USA.

Kao, E.P.C. (1974). A note on the first two moments of times in transient states in a semi-Markov process. *Journal of Applied Probability*, *11*(1), 193-198.

Kemeny, J.G., & Snell, J.L. (1976). *Finite Markov chains: With a new appendix" Generalization of a fundamental matrix"*. Springer, New York.

Mishra, K., Trivedi, K.S., & Some, R.R. (2012). Uncertainty analysis of the remote exploration and experimentation system. *Journal of Spacecraft and Rockets*, *49*(6), 1032-1042.

Mishra, R.B., Chaturvedi, S.K., & Soni, S. (2010). Reliability prediction and FMEA/FMECA of life support system of fighter aircraft. *IIT Kharagpur Report Ref: IIT/REC/FMEA/Report No. DEBEL/RP-FMEA* Date of Issue: August 24, 2010.

Misra, K.B. (2012). *Reliability analysis and prediction: A methodology oriented treatment*. Elsevier. New York.

Pievatolo, A., & Valadè, I. (2003). UPS reliability analysis with non-exponential duration distribution. *Reliability Engineering & System Safety*, *81*(2), 183-189.

Trivedi, K.S., & Bobbio, A. (2017). *Reliability and availability engineering: Modeling, analysis, and applications*. Cambridge University Press. New York.

Yin, L., Fricks, R.M., & Trivedi, K.S. (2002). Application of semi-Markov process and CTMC to evaluation of UPS system availability. In *Annual Reliability and Maintainability Symposium. 2002 Proceedings (Cat. No. 02CH37318)* (pp. 584-591). IEEE. Seattle, WA, USA.